Augmented Reality Imaging for Robot-Assisted Partial Nephrectomy Surgery

Philip Edgcumbe[1], Rohit Singla[2(✉)], Philip Pratt[3], Caitlin Schneider[2], Christopher Nguan[4], and Robert Rohling[2,5]

[1] MD/PhD Program, University of British Columbia, Vancouver, BC, Canada
edgcumbe@ece.ubc.ca
[2] Electrical and Computer Engineering, University of British Columbia, Vancouver, BC, Canada
{rsingla, rohling}@ece.ubc.ca
[3] Surgery and Cancer, Faculty of Medicine, Imperial College London, London, UK
[4] Urologic Sciences, University of British Columbia, Vancouver, BC, Canada
[5] Mechanical Engineering, University of British Columbia, Vancouver, BC, Canada

Abstract. Laparoscopic partial nephrectomy (LPN) is a standard of care for small kidney cancer tumours. A successful LPN is the complete excision of the kidney tumour while preserving as much of the non-cancerous kidney as possible. This is a challenging procedure because the surgeon has a limited field of view and reduced or no haptic feedback while performing delicate excisions as fast as possible. This work introduces and evaluates a novel surgical navigation marker called the Dynamic Augmented Reality Tracker (DART). The DART is used in a novel intra-operative augmented reality ultrasound navigation system (ARUNS) for robot-assisted minimally invasive surgery to overcome some of these challenges. The DART is inserted into a kidney and the DART and pick-up laparoscopic ultrasound transducer are tracked during an intra-operative freehand ultrasound scan of the tumour. After ultrasound, the system continues to track the DART and display the segmented 3D tumour and location of surgical instruments relative to the tumour throughout the surgery. The ultrasound point reconstruction root mean squared error (RMSE) was 0.9 mm, the RMSE of tracking the da Vinci surgical instruments was 1.5 mm and the total system RMSE, which includes ultrasound imaging and da Vinci kinematic instrument tracking, was 5.1 mm. The system was evaluated by an expert surgeon who used the DART and ARUNS to excise a tumour from a kidney phantom. This work serves as a preliminary evaluation in anticipation of further refinement and validation *in vivo*.

Keywords: Augmented reality · Robot-assisted laparoscopic surgery · Ultrasound imaging

P. Edgcumbe and R. Singla—These authors are both first authors and have contributed equally to this work.

G. Zheng et al. (Eds.): MIAR 2016, LNCS 9805, pp. 139–150, 2016.
DOI: 10.1007/978-3-319-43775-0_13

1 Introduction

Minimally invasive surgery (MIS) is growing in popularity for many types of abdominal surgery. Advantages of MIS include smaller incisions, less post-operative pain and shorter recovery times after surgery. However, MIS also has shortcomings such as reduced dexterity, limited haptic feedback, a limited field of view and poor depth perception, particularly with a monocular camera, for the surgeon [1]. This paper proposes the Dynamic Augmented Reality Tracker (DART), a custom-designed surgical navigation marker, to facilitate tumour-centric augmented reality. In particular, the DART is used in an intra-operative augmented reality ultrasound navigation system (ARUNS) that was built to overcome some of the shortcomings of MIS and to maximize the usefulness of laparoscopic ultrasound (LUS) during surgery. Surgeons use LUS as it is a real-time, non-ionizing, low-cost and intra-operative imaging modality. The system is designed for use in partial nephrectomy surgery in order to reduce the positive margin rate, the volume of healthy kidney tissue that is removed, warm ischemia time and total operating time. Maximizing healthy kidney tissue [2] and having a warm ischemia time of less than 30 min [3] results in better retention of kidney function. The purpose of this paper is to present and evaluate the DART and ARUNS in the context of a robot-assisted partial nephrectomy (RAPN) surgery in a laboratory setting.

According to a recent survey of European urologists performing RAPN, the majority use LUS and 86 % expect that augmented reality (AR) during RAPN will be useful in the future [4]. Furthermore, 82 % of surgeons practising endoscopy expect an increase in the use of LUS in the future [5]. However, in most kidney surgeries the ultrasound image is only displayed during the ultrasound scanning stage which occurs after kidney exposure and before the excision of the tumour. Displaying previously acquired ultrasound images requires that the ultrasound images be registered to the surface where the images were taken so that the surgeon sees the images moving with the organ. Tracking the surface of the smooth kidney is difficult [6].

In the context of RAPN, the DART (Fig. 1) is the proposed solution for tracking the local kidney surface and displaying the LUS ultrasound images. The surgeon places the DART in the kidney and performs a freehand ultrasound scan of the kidney and tumour. During this scan, both the DART and LUS are optically tracked. A 3D model of the tumour in the DART coordinate system is generated using optical tracking information and ultrasound segmentation. The positions of the surgical instruments relative to the tumour are displayed to the surgeon as direct AR, in two virtual camera viewpoints, and as a colour-coded warning system that alerts the surgeon if his/her instruments come dangerously close to the tumour. These two orthogonal virtual camera viewpoints, called the top and side views, are displayed to provide the surgeon with a better understanding of the location of the surgical instruments relative to the tumour. Furthermore, a guiding principle in the design of the ARUNS and introduction of virtual camera viewpoints is that surgeons generally dislike direct graphical overlays that obscure the surgical field and prefer simple stylized graphics placed beside the surgical scene [7]. The ARUNS relies on a tumour-centric tracking paradigm where ultrasound, camera, surgical instruments and DART are all related via relative, not absolute, 6-DOF tracking to maximize accuracy of the guidance.

Related work preceded ARUNS. Reviews by Lango et al. [8] and Hughes-Hallett et al. [9] summarize the significant amount of work that has already been done in the field of LUS and image-guided abdominal soft tissue surgery. Noteworthy augmented reality LUS research includes electromagnetically-tracked ultrasound for a kidney phantom model resection [10], optical tracking of the LUS for the first use of registered intra-operative ultrasound overlay in in vivo trans-anal surgery [11] and RAPN [12]. Cheung et al. showed that AR ultrasound shortens planning time [10] and Hughes-Hallett et al. used optically registered LUS to account for intra-operative tissue deformation and displayed freehand 3D reconstruction of the ultrasound image on the operative view [13]. Teber et al. previously developed a real-time AR display of the kidney tumour for the execution phase of LPNs. They employed landmark-based registration of the pre-operative segmented CT and intra-operative field of view and maintained the registration by tracking navigational aids that the surgeon had placed into the kidney [14].

The main novelties here are the invention of the DART, the tumour-centric tracking in the ARUNS, and the virtual camera display of the LUS-generated 3D tumour model and the positions of the surgical instruments relative to the tumour throughout the surgery. The ARUNS is broadly applicable to MIS and, in this first iteration, has been designed for RAPN with the da Vinci S® and Si® surgical systems (Intuitive Surgical, Sunnyvale, CA). The DART and ARUNS were tested through a user study in which an expert surgeon excised a tumour from a phantom model of a kidney tumour.

2 Materials and Methods

The DART (Fig. 1) is designed in Solidworks (Waltham, MA) and 3D printed in stainless steel at a low cost of $26 USD each to enable sterilization by autoclave (Xometry, Gaithersburg, MD). The DART can be inserted via the surgical assistant's

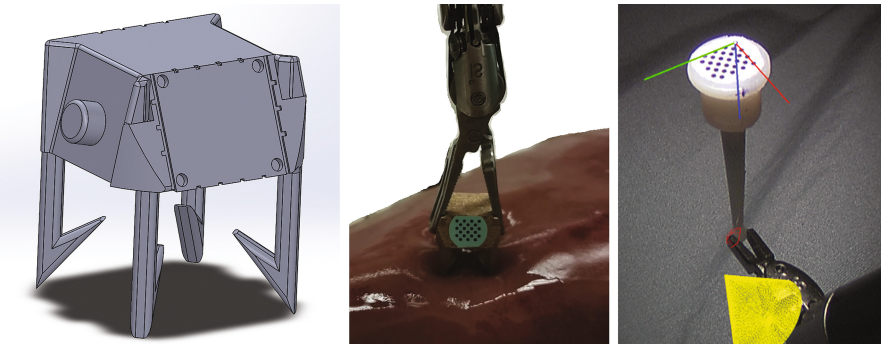

Fig. 1. The DART with repeatable grasp (left); the DART with KeyDot® marker as it is inserted into an ex vivo porcine kidney (centre); and display of modified DART for total system error analysis (right). The red circle is the centre of the pinhead as determined by ultrasound calibration and KeyDot® tracking. The vertex of the yellow cone is the location of the pinhead as determined by da Vinci surgical instrument kinematics. (Color figure online)

12 mm trocar, has a flat surface for placement of the KeyDot® optical marker [12], and can be picked up in a repeatable manner by the da Vinci Pro-Grasp™ [15]. One advantage of the repeatable grasp is that there is a fixed transform from the DART to the surgical instrument. This fixed transform means it is theoretically possible to perform da Vinci kinematic calibration by simply grasping the DART. As well, the DART facilitates a unique tumour-centric tracking system for the ARUNS. The accuracy of the generated tumour model displayed to the surgeon relies on the assumptions that the DART is fixed relative to the tumour and local tissue deformation does not occur. To that end, the DART includes legs with barbed hooks of length 10 mm that are intended to anchor it in a fixed position relative to the tumour.

The LUS transducer is designed for robot-assisted minimally invasive surgeries [15]. It has a 10 MHz 28 mm linear array and it is compatible with the Ultrasonix ultrasound machine (Analogic, Richmond, BC, Canada). The KeyDot® optical markers on the LUS transducer and DART are approved for human use (Key Surgical Inc., Eden Prairie, MN, USA). ITK-Snap [16] and Gmsh [17] are used for ultrasound segmentation and model generation. The user study is performed with the da Vinci Si® (Intuitive Surgical, Sunnyvale, CA), using the Pro-Grasp™ instrument and Monopolar curved scissors.

10–30 mm spherical inclusions at a depth of approximately 20 mm in cylindrical PVC white phantoms with a curved top surface are created using Super Soft Plastic and white colour (M-F Manufacturing, Fort Worth, TX). The phantom's elastic modulus is 15 kPa, which is consistent with the reported elastic modulus for human kidneys [18].

2.1 Calibration and Accuracy Tests

There are several components in the ARUNS system that require calibration. These include the ultrasound tracking and da Vinci kinematic chain. The purpose of the ultrasound calibration is to calculate the transformation from the linear array of the ultrasound to the KeyDot® marker asymmetrical grid of circular dot patterns [12] on the LUS transducer. The da Vinci kinematic chain calibration provides an accurate camera to tooltip transformation and corrects for inaccuracies in the da Vinci set up joint encoders, which are locked in place at the beginning of each operation.

During ultrasound calibration, optical tracking of the KeyDots®, and 3D ultrasound reconstruction are performed as described previously [12]. Ultrasound calibration accuracy is determined by imaging a pinhead in a water bath from 10 different ultrasound poses. The root mean squared error (RMSE), calculated as the Euclidian distance from each pinhead point to the centroid of the pinhead points, is calculated.

The camera is calibrated using the Caltech Camera Calibration toolbox [19]. The tooltip arm is a 12-foot-long, 13-DOF kinematic chain with absolute tracking accuracy of approximately 50 mm and relative tracking accuracy of 1 mm [20]. Thus, for accurate camera to tooltip tracking, it is necessary to perform da Vinci kinematic calibration and register the camera coordinate system to the robot coordinate system. This is achieved via registration of 14 pairs of points, one in the camera coordinate and one in the robot coordinate system. To generate each pair of points the KeyDot® is moved to a unique location and at each location the surgical instrument tip touches the

origin of the KeyDot®. In turn, a leave-one-out error for each of the 14 pairs is calculated based on a registration of the other 13 pairs. The RMSE of those 14 errors are reported.

Finally, to characterize the accuracy of the overall system, a modified DART is designed with a flat top and 2.5 mm pinhead (to simulate the tumour centre) rigidly attached exactly 25 mm below the DART surface. A model of the pinhead is generated in the DART coordinate system. Next, the da Vinci surgical instrument is used to pick up the pinhead (Fig. 1). The instrument's location in the DART coordinate system is recorded. The error is calculated as the distance between the pinhead centroid and the surgical instrument. This measure meets the goal of providing user feedback on tool-to-tumour distance. The RMSE of 10 different poses is reported.

2.2 Theory

When using the ARUNS, the surgeon sees the tumour and tooltips via the direct camera feed and via virtual cameras that appear fixed relative to the real camera. The underlying linear algebra that makes this possible is presented in this section.

The abbreviations for the coordinate frames of the ARUNS (Fig. 2) are listed here: Pick-up LUS transducer (*P*), DART (*D*), ultrasound image (*U*), surgical instrument (*I*), camera (*C*) and virtual cameras (*VC*). In the equations in this section, T is a 4×4

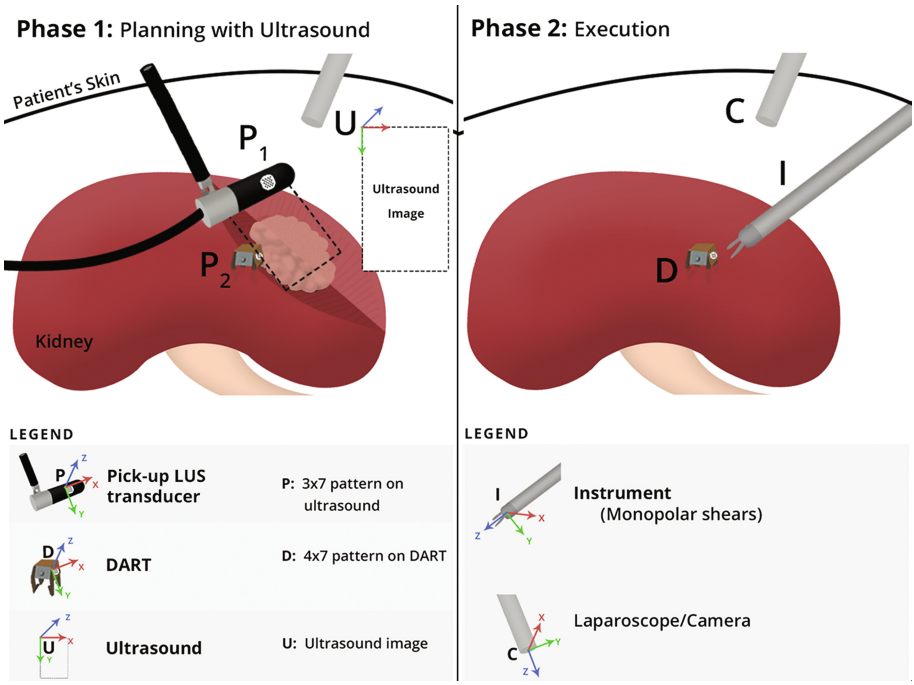

Fig. 2. System configuration with labeled coordinate frames and components for both phases.

transformation matrix, the subscript is the initial coordinate frame, the superscript is the resulting coordinate frame, the subscript of the coordinate frame subscript *o* indicates the frame at time = 0, and the camera uses the OpenCV coordinate system convention.

The ultrasound images and the locations of the da Vinci surgical instrument tooltips are transformed into the DART coordinate system via Eqs. 1 and 2 respectively:

$$^{D}T_{U} = {}^{D}T_{C} * {}^{C}T_{P} * {}^{P}T_{U} \tag{1}$$

$$^{D}T_{I} = {}^{D}T_{C} * {}^{C}T_{I} \tag{2}$$

$^{P}T_{U}$ is determined by ultrasound calibration and $^{D}T_{C}$ and $^{C}T_{P}$ are determined by optical tracking of the KeyDots® on the DART and pick-up LUS transducer respectively. $^{C}T_{I}$ is determined via the da Vinci kinematic chain from tooltip to camera.

The transformations from the virtual camera coordinate systems to the initial DART coordinate system, $^{Do}T_{VC}$, are calculated as translational and rotational components. The translations are a pre-set constant that determines the distance between the tumour and virtual cameras. The rotations are pre-set orthogonal rotations around the y and x axes of the camera. When the DART moves, a new transformation from virtual camera to the DART at time t, $^{D}T_{VC}$, is calculated as follows:

$$^{D}T_{Do} = {}^{D}T_{C} * {}^{C}T_{Co} * {}^{Co}T_{Do} \tag{3}$$

$$^{D}T_{VC} = {}^{D}T_{Do} * {}^{Do}T_{VC} \tag{4}$$

2.3 Principle of Operation

The DART placement, tracked ultrasound scan and model generation occur only in the planning phase. The augmented reality step occurs in both planning (phase 1) and execution (phase 2). The surgeon's console view is shown in Fig. 3. The step-by-step instructions for ARUNS' usage are below:

1. *DART placement*: The DART is placed into the kidney near to the tumour (Fig. 1).
2. *Tracked ultrasound scan:* During the freehand ultrasound scan of the kidney, the LUS transducer and DART KeyDot® markers are optically tracked and synchronised ultrasound images are recorded. 3D volume reconstruction is performed [21].
3. *Model generation:* A 3D model of the kidney tumour is created via manual tumour segmentation of the 3D ultrasound volume.
4. *Augmented reality:* In addition to the regular surgical scene view, orthogonal viewpoints and one direct AR image of the operative scene are displayed to the surgeon in real-time. The viewpoints include rendered tumour and tooltips, shown from the top view and side view, relative to the real camera. The views both face the centroid of the tumour and remain fixed relative to the real camera. The tumour and tooltips are continuously rendered as the DART moves. The rendering also displays the movement of the tumour in the virtual viewpoints.

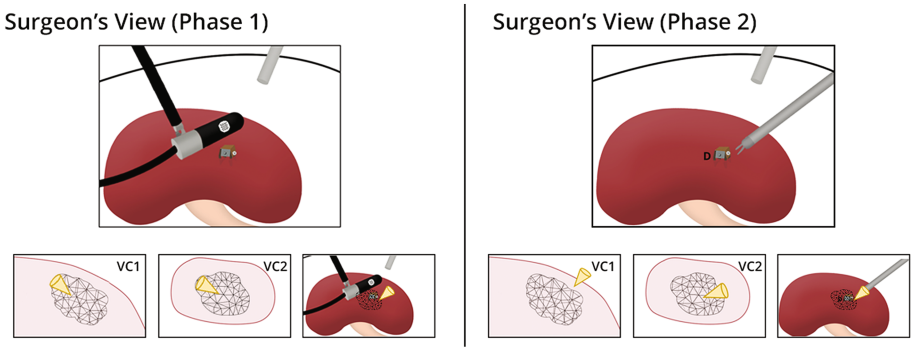

Fig. 3. The surgeon's view during the phases of the surgery. VC1 and VC2 are the orthogonal virtual camera viewpoints for top and side views. Refer to Fig. 2's legend.

5. *Tumour excision*: During the excision of the tumour, if the da Vinci surgical instrument tooltips come within a set threshold distance of the centroid of the tumour the viewpoints flash red to warn the surgeon he/she is approaching the tumour. Last, the DART is removed together with the tumour and surrounding tissue.

2.4 Surgeon User Study

One expert urological surgeon versed in robot-assisted partial nephrectomies participated in the study. The goal of the user study was to evaluate the ARUNS in a simulated RAPN surgery. In the first case, the surgeon was only given the LUS transducer. In the second case, the surgeon was given the LUS transducer and the ARUNS (LUS+ARUNS). The surgeon spent 20 min familiarizing himself with the user interface of the LUS+ARUNS system after which he was given the phantom for resection and the simulated surgery started. The phantoms provided in each case had inclusions that were purposefully unique in shape and location, limiting the surgeon's ability to learn from one case to the other. The AR overlay and orthogonal virtual camera viewpoints are placed at the bottom of the surgeon's screen using TilePro® (Figs. 3 and 4). At the end of the user study, the surgeon answered a questionnaire in which he provided feedback about both cases and both systems. The survey included questions regarding usability and helpfulness of each system.

During the planning phase of both the LUS and LUS+ARUNS cases, the surgeon marked the phantom's surface with the tip of a permanent marker held by the monopolar curved scissors. This simulated the use of electrocautery to mark the kidney surface in surgery. In both the LUS and LUS+ARUNS cases, the surgeon started the execution phase immediately after he finished the planning phase. During the execution phase he used the da Vinci surgical instruments and did not use the LUS.

The LUS+ARUNS tumour model and orthogonal virtual viewpoints were enabled at the start of the planning stage. This was possible because, for this user study, the tumour was scanned and manually segmented prior to the start of the planning phase.

The volume of excised tissue was recorded after subtracting the tissue between the top of the tumour and the tissue surface. The ratio of excised tissue to tumour volume was also recorded. The excised tissue mass was cut into 10 mm slices to determine margin status and size.

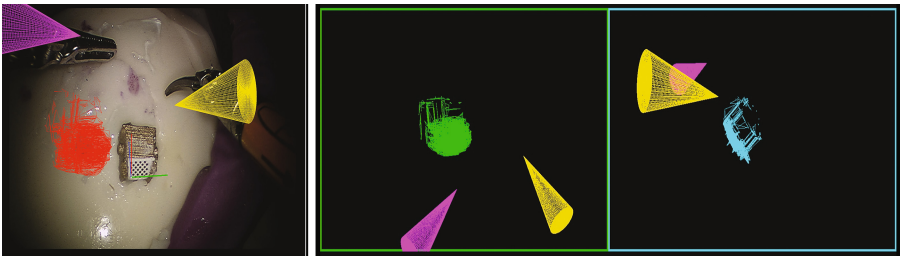

Fig. 4. The direct AR (left) and virtual camera viewpoints (middle and right) that are shown to the surgeon using LUS+ARUNS in addition to his/her normal view. The middle pane is the top-down view and right pane is the side view of the surgical scene.

3 Results

3.1 Calibration and Accuracy Tests

The ultrasound calibration result of the pinhead reconstruction relative accuracy was 0.9 mm. Over the course of capturing the 10 ultrasound images of the pinhead, the ultrasound transducer covered a range of 16 × 10 × 19 mm. The da Vinci kinematic calibration and camera-to-tooltip error was 1.5 mm. The lowest single error was 0.6 mm. The correction factor matrix associated with the 0.6 mm error was used for the rest of the experiment. The overall system error was 5.1 mm.

3.2 Surgeon User Study

For the LUS only case, the planning and execution times were 2 min and 10 min 45 s, respectively. The excised tissue volume was 24 cm^3 and the volume of the tumour was 4 cm^3. Thus, the excised tissue volume to tumour volume ratio was 6:1. There was a gross margin and a separate microscopically (<1 mm) positive margin. The largest negative margin size was 24 mm.

For the LUS+ARUNS case, the planning and execution time were 1 min 57 s and 7 min 30 s respectively. The excised tissue volume was 16.5 cm^3, and the volume of the tumour was 5.5 cm^3. Thus, the excised tissue volume to tumour volume ratio was 3:1. There was a gross and a separate microscopically positive margin. The largest negative margin size was 12 mm. For both cases, the tumour was endophytic and the surgeon rated the R.E.N.A.L nephrometry score [22] as 12. In other words, a very difficult surgery was simulated.

After the user study, the surgeon reported that the ARUNS+LUS case provided more information for visualization of the tumour in the planning phase. The surgeon preferred the ARUNS+LUS case over the LUS case for visualizing the tumour in the

execution phase. General comments about the ARUNS+LUS system include that the most useful guidance cue was that the screen flashed red once the instruments got to within a certain distance of the centre of the tumour. The warning aided the surgeon in avoiding the tumour and minimizing the healthy tissue excised. The surgeon found the top-down view easier to interpret than the side view. Video clips from the surgical resection performed for the ARUNS+LUS are included as supplementary material.

4 Discussion

The success of image-guided surgical systems is largely dependent on their accuracy, usability and the clinical need for the extra image guidance. Each of those aspects of the ARUNS will be addressed in turn in the discussion.

Both the ultrasound pinhead reconstruction precision error of 0.9 mm and the error of 1.5 mm for the da Vinci kinematics were consistent with error for similar experiments that have been reported in the literature of 1.2 mm [23] and 1.0 mm [20] respectively. The larger error in ARUNS may be because the gold standard used were optically tracked KeyDot® markers as opposed to an Optotrak® 3020 stylus (Northern Digital Instruments, Waterloo, ON, Canada), which has a reported tip error of 0.25 mm [20]. Given an ultrasound error of 0.9 mm and da Vinci kinematics error of 1.5 mm, the measured total system error of the ARUNS of 5.1 mm can be reduced through further refinement and testing. There is still error from optical tracking of both the LUS and the DART, manual pinhead segmentation, and an imprecise technique for touching the pinhead with the surgical instruments. Given that one of the end goals for ARUNS is to increase the amount of healthy kidney that is spared, it is important to reduce the total system error further. The standard of care recommendation for a kidney tumour resection is to leave a safety margin of 5 mm [3].

In terms of usability, the ARUNS orthogonal virtual camera viewpoint is different to other image guidance systems for abdominal surgery. The advantage of the orthogonal viewpoints is that it provides the surgeon a perspective they would not normally have without occluding the surgeon's view of the operative field. An additional advantage to the virtual viewpoints approach is that the lag, inevitably introduced by an image guidance system with graphical rendering, is much less of a distraction in the orthogonal view as opposed to the direct overlay view. However, further work is required in ARUNS for the positioning of the views, as the surgeon had difficulty orienting himself relative to given views. Additional simplistic cues such as rendering the camera, showing the centre line axis of the virtual viewpoints or letting the surgeon set the pose of the virtual viewpoints could help with minimize these issues. Using a colour gradient to represent the distance of the instrument to the tumour could improve the warning cue given to the surgeon as well.

The ARUNS differs from the work of Teber et al. [14] in the following ways: (1) only one surgical navigation marker, the DART, is inserted into the kidney, (2) the augmented reality image displayed is a 3D representation of the tumour generated by the intra-operative LUS scan, and (3) the surgical instruments and the display is presented to the surgeon via two orthogonal virtual camera viewpoints and a direct AR overlay (Fig. 4).

The ultimate goal is that the ARUNS will be used for human surgeries. To achieve that goal, the issues of ultrasound segmentation, possible tissue deformation relative to the DART, renal artery clamping, blood occlusion and seeding risk will have to be addressed. For simplicity, manual segmentation was performed. In practice, segmentation time can be minimised using (semi-)automatic algorithms that exist or using a bounding sphere approach for complex tumour geometry. However, *in vivo* automatic segmentation of tumours is more difficult than segmentation of phantoms. To account for tissue deformation, a FEM model of the tumour may be required [24] plus real-time surface geometry reconstruction. For renal artery clamping, the main issue is that, to minimize warm ischemia time, the ultrasound imaging should be performed prior to renal artery clamping. The shape of the kidney and tumour change when the perfusion pressure drops to zero. Insertion of the DART into the kidney yields a potential risk of seeding. According to preliminary tests, this may be prevented by using the stainless steel DART with electrocautery. It is also feasible that a range of DART geometries be available to the surgeon depending on tumour depth: long barbs for deep tumours, short barbs for shallow tumours and adhesive fixation for superficial tumours. Blood occlusion of the DART pattern can alleviated through an omniphobic coating to repel blood [25].

5 Future Work and Conclusion

Future studies are required with more users and more trials of the system. This will provide more robust results than the single surgeon/single phantom study performed, as well as provide a clearer understanding on usability and preference. For these studies, subsystem improvements and more rigorous validation can be performed.

The DART and ARUNS offer many interesting avenues for future research. One novel addition would be the incorporation of surface reconstruction. This can be facilitated by structured light using, for example, laser-based solutions [26] or projector-based solutions like the Pico Lantern [27]. A reconstructed surface mesh could be displayed in the orthogonal views to provide further depth cues. Furthermore, the surface could be used to provide the surgeon a true top-down view, as opposed to a view that is orthogonal to their camera viewpoint. Future work for ARUNS could also be the integration of the Pico Lantern for AR in MIS, such as the projection of the tumour outline onto the surface of the kidney. Using the generated surface mesh, an outline of the tumour from the perspective of the camera can be calculated and projected back onto the surface using the tracked projector.

There are also further extensions possible for the DART design and AR display. For example, customised tumour-based DARTs can be created from pre-operative imaging prior to surgery to handle tumours of varying geometries. For protruding tumours, instead of tracking the KeyDot® pattern on the DART optically, it could be used to brand a trackable pattern on the surface using electrocautery. Also, by using several unique DARTs, surgeons could insert them throughout surgery to provide persistent AR and overcome the line-of-sight issues. The virtual views are not limited to rendering one tumour mesh and the da Vinci tools. In practice, the AR display can be extended to include any model including blood vessels and other subsurface structures from pre-operative and intra-operative imaging sources. Leveraging the instrument tracking,

a display of the path taken and the projected tool path can be shown as further guidance cues. The virtual views also let the surgeon see beyond their field of view, and localize tools or devices such as the LUS probe. These applications are all enabled by the relative tracking paradigm created by the DART. Finally, the DART and ARUNS concepts can be generalised to provide image guidance for standard non-robotic laparoscopy. In conclusion, the ARUNS is an innovative approach to surgical navigation for minimally invasive surgery and further investigation and user studies are warranted.

Acknowledgements. The authors gratefully thank Andrew Wiles of Northern Digital Inc. for support; Prof. Tim Salcudean for providing infrastructure and advice; Denise Kwok for graphics; and funding from the CIHR Vanier Scholarship, VCH-CIHR-UBC MD/PhD Studentship Award and the NSERC CGS-M Award.

References

1. Elhage, O., Murphy, D., Challacombe, B., Shortland, A., Dasgupta, P.: Ergonomics in minimally invasive surgery. Int. J. Clin. Pract. **61**(2), 186–188 (2007)
2. Sutherland, S.E., Resnick, M.I., Maclennan, G.T., Goldman, H.B.: Does the size of the surgical margin in partial nephrectomy for renal cell cancer really matter? J. Urol. **167**(1), 61–64 (2002)
3. Gill, I.S., Desai, M.M., Kaouk, J.H., Meraney, A.M., Murphy, D.P., Sung, G.T., Novick, A.C.: Laparoscopic partial nephrectomy for renal tumor: duplicating open surgical techniques. J. Urol. **167**(2), 469–476 (2002)
4. Hughes-Hallett, A., Mayer, E.K., Pratt, P., Mottrie, A., Darzi, A., Vale, J.: The current and future use of imaging in urological robotic surgery: a survey of the European Association of Robotic Urological Surgeons. Int. J. Med. Robot. Comput. Assist. Surg. **11**(1), 8–14 (2015)
5. Våpenstad, C., Rethy, A., Langø, T., Selbekk, T., Ystgaard, B., Hernes, T.A.N., Mårvik, R.: Laparoscopic ultrasound: a survey of its current and future use, requirements, and integration with navigation technology. Surg. Endosc. **24**(12), 2944–2953 (2010)
6. Su, L.M., Vagvolgyi, B.P., Agarwal, R., Reiley, C.E., Taylor, R.H., Hager, G.D.: Augmented reality during robot-assisted laparoscopic partial nephrectomy: toward real-time 3D-CT to stereoscopic video registration. Urology **73**(4), 896–900 (2009)
7. Schneider, C.M., Dachs II, G.W., Hasser, C.J., Choti, M.A., DiMaio, S.P., Taylor, R.H.: Robot-assisted laparoscopic ultrasound. In: Navab, N., Jannin, P. (eds.) IPCAI 2010. LNCS, vol. 6135, pp. 67–80. Springer, Heidelberg (2010)
8. Langø, T., Vijayan, S., Rethy, A., Våpenstad, C., Solberg, O.V., Mårvik, R., Johnsen, G., Hernes, T.N.: Navigated laparoscopic ultrasound in abdominal soft tissue surgery: technological overview and perspectives. Int. J. Comput. Assist. Radiol. Surg. **7**(4), 585–599 (2012)
9. Hughes-Hallett, A., Mayer, E.K., Marcus, H.J., Cundy, T.P., Pratt, P.J., Darzi, A.W.: Augmented reality partial nephrectomy: examining the current status and future perspectives. Urology **83**(2), 266–273 (2014)
10. Cheung, C.L., Wedlake, C., Moore, J., Pautler, S.E., Peters, T.M.: Fused video and ultrasound images for minimally invasive partial nephrectomy: a phantom study. In: Jiang, T., Navab, N., Pluim, J.P.W., Viergever, M.A. (eds.) MICCAI 2010. LNCS, vol. 6363, pp. 408–415. Springer, Heidelberg (2010)

11. Pratt, P., Di Marco, A., Payne, C., Darzi, A., Yang, G.Z.: Intraoperative ultrasound guidance for transanal endoscopic microsurgery. In: Ayache, N., Delingette, H., Golland, P., Mori, K. (eds.) MICCAI 2010. LNCS, vol. 7510, pp. 463–470. Springer, Heidelberg (2012)
12. Pratt, P., Jaeger, A., Hughes-Hallett, A., Mayer, E., Vale, J., Darzi, A., Peters, T., Yang, G.Z.: Robust ultrasound probe tracking: initial clinical experiences during robot-assisted partial nephrectomy. Int. J. Comput. Assist. Radiol. Surg. **10**(12), 1905–1913 (2015)
13. Hughes-Hallett, A., Pratt, P., Dilley, J., Vale, J., Darzi, A., Mayer, E.: Augmented reality: 3D image-guided surgery. Cancer Imaging **15**(Suppl. 1), O8 (2015)
14. Teber, D., Guven, S., Simpfendörfer, T., Baumhauer, M., Güven, E.O., Yencilek, F., Gözen, A.S., Rassweiler, J.: Augmented reality: a new tool to improve surgical accuracy during laparoscopic partial nephrectomy? Preliminary in vitro and in vivo results. Eur. Urol. **56**(2), 332–338 (2009)
15. Schneider, C., Guerrero, J., Nguan, C., Rohling, R., Salcudean, S.: Intra-operative "Pick-Up" ultrasound for robot assisted surgery with vessel extraction and registration: a feasibility study. In: Taylor, R.H., Yang, G.-Z. (eds.) IPCAI 2011. LNCS, vol. 6689, pp. 122–132. Springer, Heidelberg (2011)
16. Yushkevich, P.A., Piven, J., Hazlett, H.C., Smith, R.G., Ho, S., Gee, J.C., Gerig, G.: User-guided 3D active contour segmentation of anatomical structures: significantly improved efficiency and reliability. Neuroimage **31**(3), 1116–1128 (2006)
17. Geuzaine, C., Remacle, J.F.: Gmsh: a 3-D finite element mesh generator with built-in pre- and post-processing facilities. Int. J. Numer. Methods Eng. **79**(11), 1309–1331 (2009)
18. Grenier, N., Gennisson, J.L., Cornelis, F., Le Bras, Y., Couzi, L.: Renal ultrasound elastography. Diagn. Interv. Imaging **94**(5), 545–550 (2013)
19. Bouguet, J.Y.: Camera calibration toolbox for matlab (2004)
20. Kwartowitz, D.M., Herrell, S.D., Galloway, R.L.: Toward image-guided robotic surgery: determining intrinsic accuracy of the da Vinci robot. Int. J. Comput. Assist. Radiol. Surg. **1**(3), 157–165 (2006)
21. Gooding, M.J., Kennedy, S., Noble, J.A.: Volume segmentation and reconstruction from freehand three-dimensional ultrasound data with application to ovarian follicle measurement. Ultrasound Med. Biol. **34**(2), 183–195 (2008)
22. Kutikov, A., Uzzo, R.G.: The RENAL nephrometry score: a comprehensive standardized system for quantitating renal tumor size, location and depth. J. Urol. **182**(3), 844–853 (2009)
23. Edgcumbe, P., Nguan, C., Rohling, R.: Calibration and stereo tracking of a laparoscopic ultrasound transducer for augmented reality in surgery. In: Liao, H., Linte, C.A., Masamune, K., Peters, T.M., Zheng, G. (eds.) MIAR 2013 and AE-CAI 2013. LNCS, vol. 8090, pp. 258–267. Springer, Heidelberg (2013)
24. Camara, M., Mayer, E., Darzi, A., Pratt, P.: Soft tissue deformation for surgical simulation: a position-based dynamics approach. Int. J. Comput. Assist. Radiol. Surg. **11**(6), 919–928 (2016)
25. Leslie, D.C., Waterhouse, A., Berthet, J.B., Valentin, T.M., Watters, A.L., Jain, A., Kim, P., Hatton, B.D., Nedder, A., Donovan, K., Super, E.H.: A bioinspired omniphobic surface coating on medical devices prevents thrombosis and biofouling. Nat. Biotechnol. **32**(11), 1134–1140 (2014)
26. Lin, J., Clancy, N.T., Stoyanov, D., Elson, D.S.: Tissue surface reconstruction aided by local normal information using a self-calibrated endoscopic structured light system. In: Navab, N., Hornegger, J., Wells, W.M., Frangi, A.F. (eds.) MICCAI 2015. LNCS, vol. 9349, pp. 405–412. Springer, Heidelberg (2015)
27. Edgcumbe, P., Pratt, P., Yang, G.Z., Nguan, C., Rohling, R.: Pico Lantern: surface reconstruction and augmented reality in laparoscopic surgery using a pick-up laser projector. Med. Image Anal. **25**(1), 95–102 (2015)